Posttranslational Modification of Vesicular Stomatitis Virus Glycoprotein, but Not JNK Inhibition, Is the Antiviral Mechanism of SP600125

Sabrina Marozin,[a] Jennifer Altomonte,[a] Sibylle Apfel,[a] Phat X. Dinh,[b] Enrico N. De Toni,[c] Antonia Rizzani,[c] Andreas Nüssler,[d] Nobuyuki Kato,[e] Roland M. Schmid,[a] Asit K. Pattnaik,[b] and Oliver Ebert[a]

Department of Medicine, Klinikum rechts der Isar, Technical University of Munich, Munich, Germany[a]; School of Veterinary Medicine and Biomedical Sciences and the Nebraska Center for Virology, University of Nebraska—Lincoln, Lincoln, Nebraska, USA[b]; Department of Medicine 2, University Hospital Grosshadern, University of Munich, Munich, Germany[c]; Department of Traumatology, Klinikum rechts der Isar, Technical University of Munich, Munich, Germany[d]; and Department of Molecular Biology, Okayama University Graduate School of Medicine, Dentistry, and Pharmaceutical Sciences, Okayama, Japan[e]

Vesicular stomatitis virus (VSV), a negative-sense single-stranded-RNA rhabdovirus, is an extremely promising oncolytic agent for cancer treatment. Since oncolytic virotherapy is moving closer to clinical application, potentially synergistic combinations of oncolytic viruses and molecularly targeted antitumor agents are becoming a meaningful strategy for cancer treatment. Mitogen-activated protein kinase (MAPK) inhibitors have been shown to impair liver cell proliferation and tumor development, suggesting their potential use as therapeutic agents for hepatocellular carcinoma (HCC). In this work, we show that the impairment of MAPK *in vitro* did not interfere with the oncolytic properties of VSV in HCC cell lines. Moreover, the administration of MAPK inhibitors did not restore the responsiveness of HCC cells to alpha/beta interferon (IFN-α/β). In contrast to previous reports, we show that JNK inhibition by the inhibitor SP600125 is not responsible for VSV attenuation in HCC cells and that this compound acts by causing a posttranslational modification of the viral glycoprotein.

esicular stomatitis virus (VSV), a negative-sense single-stranded-RNA rhabdovirus, which has inherent tumor specificity for replication due to attenuated type I interferon (IFN) (IFN-α/β) responses in most tumor cells, is an extremely promising oncolytic agent for cancer treatment (52, 53). A characterization of cellular events supporting VSV oncolysis is important for an understanding of virus-cell interactions in infected tumor cells, including hepatocellular carcinoma (HCC). Moreover, an investigation of the host cell determinants of permissiveness to VSV infection is essential for the development of viral vectors with enhanced oncolytic properties for HCC.

The c-Jun N-terminal kinases (JNKs) belong to the superfamily of mitogen-activated protein kinases (MAPKs), which also includes p38 MAPK and extracellular signal-regulated kinase (ERK) (57). MAPKs are usually involved in the regulation of cell proliferation, differentiation, and apoptosis (6, 28). JNKs are activated, together with p38 MAPK, by different stimuli, including stress factors, inflammatory cytokines, and cytotoxic and genotoxic factors and play a critical role in mediating apoptotic signaling (32). JNK and p38 MAPK signals are often deregulated during malignant transformation, and cancer cells can subvert these pathways to facilitate proliferation, survival, and invasion (4, 5, 17, 24). JNK has been reported to exert oncogenic functions in HCC, and an increased kinase activity correlates with increased tumor proliferation (8, 22). The inhibition of JNK has been shown to impair liver cell proliferation and tumor development, suggesting the potential use of these inhibitors as therapeutic agents for HCC (42).

Human HCC cells are highly resistant to tumor necrosis factor-related apoptosis-inducing ligand (TRAIL)-induced cytotoxicity (51). Interestingly, treatment with a JNK inhibitor (JNKi) (SP600125) sensitizes HCC cells to TRAIL, providing evidence that the activity of JNK is required for resistance to apoptosis in these tumors (41). Several members of different viral families ac-

tivate JNK and p38 MAPK gene-regulated cascades, in some cases resulting in the induction of apoptosis in infected cells and increased viral replication (9, 18). In particular, the activation of the JNK transduction pathway has been observed during infection with several DNA and RNA viruses, suggesting an important role in viral replication (2, 7, 10, 19). Interestingly, JNK activation is a common feature of many disparate viruses; therefore, it may represent an important target for the development of antiviral treatments. The aberrant activation of JNK is an important feature of tumorigenesis, and the constitutive activation of JNK occurs in most HCCs. Since VSV is a promising therapeutic agent against HCC, here we were interested in investigating the role of JNK in VSV oncolysis. Our studies revealed that JNK inhibition by the inhibitor SP600125 does not play any role in the attenuation of VSV in HCC cells. Rather, this compound acts by inducing a posttranslational modification of the viral glycoprotein, resulting in a significant reduction in the infectivity of the virus in these cells.

MATERIALS AND METHODS

Cell lines, primary human hepatocytes, and viruses. Two human HCC cell lines (HepG2 and Huh-7), kind gifts from Ulrich Lauer (University Hospital of Tübingen), were maintained in Dulbecco's modified Eagle's medium (DMEM) supplemented with 10% fetal bovine serum (FBS), 1% L-glutamine (200 mM), 1% penicillin-streptomycin, 1% nonessential amino acids, and 1% sodium pyruvate. Immortalized human hepatocytes

(PH5CH8) were maintained in DMEM–F-12 medium. All cell cultures were regularly tested for mycoplasma contamination. Primary human hepatocytes (PHH) were derived from patients (negative for hepatitis B virus [HBV], hepatitis C virus [HCV], and HIV) who underwent surgical resections of liver tumors. Human hepatocytes were isolated by a two-step collagenase perfusion technique followed by Percoll gradient centrifugation for purification, as previously described (44). Wild-type VSV-green fluorescent protein (GFP) was generated as previously described (14). Virus stocks were produced on BHK-21 cells and stored at −80°C. Titers were determined by a plaque assay on BHK-21 cells (14).

Western blotting. Whole-cell extracts or isolated viral pellets were run on a 7.5% SDS-PAGE gel and transferred onto nitrocellulose membranes. Total cell lysates were prepared by using Cell Lysing buffer (Cell Signaling Technology Inc., Danvers, MA) containing a protease and phosphatase inhibitor cocktail. The protein concentration in the samples was determined by using a bicinchoninic acid (BCA) protein assay kit (Promega, Madison, WI) according to the manufacturer's instructions. After blocking for 1 h with 5% skim milk–Tris-buffered saline (TBS)–Tween, membranes were blotted with the following primary antibodies (Abs) overnight at 4°C: antibodies against basal and phosphorylated forms of JNK, ERK1 and -2, and p38 MAPK (Cell Signaling); VSV-G (Abcam, Cambridge, United Kingdom); and actin (Sigma-Aldrich, Munich, Germany) and anti-VSV serum (kindly provided by Douglas Lyles). After secondary staining with anti-rabbit or anti-mouse peroxidase-conjugated Abs (Jackson ImmunoResearch Laboratories Inc., West Grove, PA), protein bands were visualized on Amersham Hyper-Max film with the ECL chemiluminescence kit as recommended by the manufacturer (Amersham, Buckinghamshire, United Kingdom).

Viral growth assays. Single infections and one-step growth curves of recombinant VSV (rVSV)-GFP were performed on PHH, immortalized human hepatocytes (PH5CH8), and the HepG2 and Huh-7 cell lines. Cells were infected at a multiplicity of infection (MOI) of 0.1 or 10 according to the experiment. After adsorption for 1 h, the monolayers were washed three times with phosphate-buffered saline (PBS), and fresh medium was added. Aliquots of culture media were collected at the indicated times postinfection. Viral titers were determined by 50% tissue culture infective dose ($TCID_{50}$) analysis and represent the averages of data from triplicate experiments. For interferon protection assays, cells were mock treated or incubated with 1,000 IU/ml of universal type I IFN (PBL Biomedical Laboratories) overnight and subsequently infected with rVSV-GFP for 16 h.

Treatment with MAPK inhibitors, DTT, and urea. Cells were seeded at 80 to 90% confluence in 24-well plates overnight. The next morning, the culture media were replaced with fresh media containing dimethyl sulfoxide (DMSO) or MAPK inhibitors at the indicated concentrations. After pretreatment for 16 h, virus infections were carried out in the presence of freshly added inhibitors. Chemicals (SB203580 [10 μM], SP600125 [25 μM], and U0126 [10 μM]) were purchased from Calbiochem-Merck (Gibbstown, NJ). For experiments with the JNK inhibitor, Huh-7 cells were pretreated with SP600125 (25 μM), and infection was allowed to proceed either in the absence or in the presence of fresh inhibitor for the entire duration of the experiment. Viral titers were determined at 24 h postinfection (hpi) by $TCID_{50}$ analysis.

Dithiothreitol (DTT) was added to semipurified virions to final concentrations of 10 and 50 mM. Samples were incubated at 56°C for 15 min. Treatment with urea was performed by the incubation of virions with 8 M urea for 10 min at room temperature (RT); direct separation on SDS-PAGE gels was applied without preheating the samples.

For the chemical cross-linking of VSV, samples of semipurified virions were incubated with SP600125 to a final concentration of 25 μM for 1 h on ice. Alternatively, cross-linking with 2% paraformaldehyde (PFA) was carried out on ice for 15 min. Samples were preheated at 56°C for 10 min and assayed by Western blotting.

Real-time PCR. Cells were infected with rVSV-GFP; cell supernatants and cell lysates were collected at the indicated time points. Cell debris was

eliminated by centrifugation and total RNA was extracted, according to the manufacturers' instructions, by using the High Pure viral RNA kit (Roche, Mannheim, Germany) and the RNeasy Plus minikit (Qiagen, Valencia, CA), respectively. The forward and reverse primers generating a 138-nucleotide DNA fragment spanning one intergenic region between the N and P genes were designed as previously reported (14). Quantitative real-time PCR was carried out with the QuantiTect Probe reverse transcription kit (Qiagen, Valencia, CA) and the Kapa SYBR Fast qPCR Fast LightCycler 480 kit (PeqLab, Erlangen, Germany), using 15 ng of the template. The relative values for mRNA extracted from cell lysates were quantified by normalizing the expression level of the gene of interest to the level of the internal housekeeping control RNA (glyceraldehyde-3-phosphate dehydrogenase [GAPDH]). The quantification of viral RNA from infected supernatants was performed by using an external standard curve.

siRNA assays. For small interfering RNA (siRNA) experiments, reverse transfection was performed by using Lipofectamine RNAiMax (Invitrogen). Cells in 24-well plates were transfected with either 100 nM scrambled siRNA or specific siRNA (100 nM) according to the manufacturer's instructions. siRNAs were synthesized by Dharmacon (Thermo Fisher Scientific). After 48 to 72 h posttransfection, cultures were infected with rVSV-GFP at an MOI of 0.1 for 16 h. Titers were determined as the $TCID_{50}$. Cell lysates from uninfected duplicate cultures were analyzed by Western blotting to assess the efficiency of RNA silencing against JNK expression. Alternatively, 48 h after siRNA transfection, cells were treated with SP600125 or with DMSO and subsequently infected with VSV at an MOI of 0.1.

Transfection of a VSV glycoprotein-encoding plasmid and evaluation of syncytium formation. The VSV-G expression plasmid (pCMV-VSV-G) was kindly provided by Dorothee von Laer, Innsbruck, Austria. One microgram of plasmid was transfected into Huh-7 cells by using Lipofectamine LTX according to the manufacturer's instructions (Invitrogen). At 8 h posttransfection, the supernatant was replaced with fresh medium containing DMSO or SP600125 (25 μM). GFP under the control of a cytomegalovirus (CMV) promoter (pCMV-C3) was used as the transfection control. The presence of SP600125 did not influence transfection efficiency rates, as observed by the level of GFP expression and the number of GFP-positive cells with or without the inhibitor. Cell-cell fusion was allowed to progress without low-pH treatment to activate fusion, as previously described (11, 48).

After 24 to 36 h, cells were fixed with ice-cold 70% ethanol for 5 to 10 min at −20°C, and nuclei were visualized by propidium iodide staining. Syncytium formation was determined by the syncytium index (SI), calculated as the number of nuclei per syncytium divided by the number of nuclei per field of view. ImageJ software (National Institutes of Health, Bethesda, MD) was used to quantify the number of nuclei.

Glycosylation analysis. Semipurified virions obtained from DMSO- or SP600125-treated cells were subjected to digestion with endoglycosidase F (PNGase F) or with endo-α-N-acetylgalactosaminidase (EndoGalNAcase) (New England BioLabs, Frankfurt am Main, Germany). Samples were incubated overnight at 37°C, according to the manufacturer's instructions. Negative-control experiments were performed with deglycosylation buffers in the absence of the respective deglycosylation enzymes.

Mass spectrometry of the modified VSV G protein. Purified VSV obtained from SP600125-treated cells was separated on an SDS-PAGE gel. Viral proteins were stained with the Coomassie staining method, using GelCode Blue Stain reagent (Thermo Scientific) according to the manufacturer's instructions. Selected bands were excised and subjected to liquid chromatography (LC)/mass spectrometry (MS) as described previously (26). Briefly, gel pieces were digested with trypsin (catalog no. V5111; Promega, Madison, WI), and the digested peptides were extracted in 5% formic acid–50% acetonitrile and separated by using a C_{18} reversed-phase LC column (Milford, MA). A Q-TOF Ultima tandem mass spectrometer coupled with a Nanoaquity high-performance liquid chromatography (HPLC) system (Waters) with electrospray ionization was used to analyze the eluting peptides. The peak lists of tandem mass spectrom-

etry (MS/MS) data were generated by using Distiller (Matrix Science, London, United Kingdom), using charge state recognition and deisotoping with the other default parameters for Q-TOF data. Database searches of the acquired MS/MS spectra using NCBI database 20100701 were performed with Mascot (v2.2.0; Matrix Science, London, United Kingdom). Mass accuracy settings were 0.15 Da for peptide masses and 0.12 Da for fragment ion masses.

Statistical analysis. Data were analyzed for statistical significance by using GraphPad Prism 5.0 (GraphPad Software, San Diego, CA). Individual data points were compared by applying a two-sided Student t test, and P values of less than 0.05 were considered statistically significant.

RESULTS

JNK, ERK, and p38 MAPK activation in malignant and nonneoplastic hepatocytes infected with VSV. To examine the activation states of JNK, ERK, and p38 MAPK upon VSV infection, HCC cells (HepG2 and Huh-7), nonneoplastic immortalized hepatocytes (PH5CH8), and primary human hepatocytes (PHH) were infected with rVSV-GFP, and lysates were collected at different hours postinfection. The activation of these molecules occurs as a result of phosphorylation; therefore, the cell lysates were analyzed by Western blotting using phospho-specific antibodies to each of these proteins. JNK activation levels increased over time and peaked at different time points, depending on the cell type (Fig. 1A). In Huh-7 cells, the level of JNK activation was at its highest at 6 hpi and remained high until 12 hpi. In HepG2 and PH5CH8 cells, we observed a gradual increase of the level of the phosphorylated JNK form up to 12 hpi. However, in PHH, JNK activation was not significant, and only a slight increase at the final time point was detected. The levels of phosphorylated ERK in HCC cell lines showed a minimal increment at around 4 to 6 hpi but remained unchanged (in Huh-7 cells) or decreased at later time points. In contrast, p38 MAPK showed a delayed activation, occurring at 12 hpi. In HCC cells, the phosphorylation of JNK is a fairly late event during VSV infection, which starts at around 4 hpi, coincident with VSV glycoprotein (VSV-G) expression. Infection with a UV-inactivated virus did not induce JNK activation (data not shown).

To determine if JNK activity is necessary for the efficient replication of VSV in cell cultures, the effect of the JNK inhibitor (JNKi) SP600125 was compared to those of the ERK inhibitor (ERKi) and the p38 MAPK inhibitor (p38i). First, cells were pretreated with various chemical inhibitors and, in the presence of fresh inhibitors, infected with rVSV-GFP. VSV growth was significantly reduced only in the presence of JNKi, and attenuation was observed for all cell types (Fig. 1B). Western blotting for phospho-JNK indicated that the JNK inhibitor specifically reduced JNK phosphorylation in VSV-infected HCC cells without interfering with ERK activation (data not shown). In PHH, the inhibitory effect was not as pronounced, and additionally, ERK appeared to be affected. Nevertheless, ERK dephosphorylation was already present in VSV-infected cultures not treated with the JNK inhibitor. Thus, our results show that in contrast to JNK, the inhibition of ERK and p38 MAPK by their specific inhibitors did not influence VSV replication.

In addition, an siRNA-mediated knockdown of JNK was performed in HCC cell lines and nonneoplastic hepatocytes to confirm the specificity of SP600125. Cells were transfected with scramble (Scr) siRNA or a pool of two different siRNAs against JNK kinases, followed by infection with rVSV-GFP. Despite a robust decrease of JNK protein levels, viral replication was not affected, and no significant differences in titers were observed (Fig. 1C, left). To further define whether the inhibition of JNK was associated with the SP600125-dependent attenuation of VSV growth, HCC cells (data for HepG2 cells are shown) were transfected with either scramble or JNK-specific siRNAs (Fig. 1C, right). Infection was carried out in the absence or presence of SP600125, and viral titers were determined 24 h later. The effective knockdown of the JNK protein was assessed by Western blotting. As shown in Fig. 1C (right), in the presence of the JNK inhibitor, both scramble siRNA- and JNK siRNA-transfected cells were equally susceptible to SP600125, supporting the observation that productive VSV infection does not require JNK.

Inhibitors of the MAPK signal do not sensitize HCC cells to type I interferon. To determine the effect of the MAPK inhibitors on type I IFN sensitivity, cells were treated with ERK, p38 MAPK, and JNK inhibitors alone or in combination with IFN-α/β, followed by VSV infection, as described above. In all cell types, the viral titers were appreciably lower in cultures treated with the JNK inhibitor than in cultures treated with DMSO. A robust attenuation of virion production upon combined treatment with SP600125 and IFN-α/β was observed, especially in PHH and in PH5CH8 cells, indicating an additive effect of type I IFN with SP600125 activity on viral replication (Fig. 2A). The inhibition of ERK and p38 MAPK did not enhance the efficacy of IFN-α/β against VSV in HCC cells (Fig. 2B and C).

SP600125 can synergistically enhance cell apoptosis in cancer cells (30, 37, 41). We excluded apoptosis as the cause of VSV growth attenuation by SP600125, since the caspase inhibitor benzyloxycarbonyl-Val-Ala-Asp(OMe)-fluoromethylketone (Z-VAD-FMK) did not block the JNK inhibitor effect on viral titers, and SP600125 did not induced apoptosis in PHH (data not shown).

Viral transcription/translation and viral budding are not altered by SP600125. To identify the specific viral process blocked by the JNK inhibitor, we examined the levels of viral RNA transcription in cells treated with SP600125. HepG2 cells as well as PHH were pretreated with DMSO or SP600125 (25 μM) and infected with VSV at an MOI of 1. Total RNAs from cell lysates were harvested at different time points (0, 2, 4, and 8 hpi) and analyzed for the presence and concentrations of genomic VSV RNA and for nucleoprotein (N) mRNA by real-time PCR. The results show that the inhibition of JNK did not interfere with VSV mRNA transcription (Fig. 3A) or genome replication in HCC or in PHH cells (Fig. 3B). Additionally, levels of the VSV G protein in SP600125-treated cells were comparable to those in control samples (Fig. 3C). Furthermore, we compared the numbers of infectious viral particles in the lysates and in the supernatants of cells treated with vehicle (DMSO), interferon (IFN), or SP600125 (JNKi). In HCC cells treated with SP600125, the numbers of infectious particles in the cell lysates were comparable to that present in the corresponding supernatants (Fig. 3D).

Virions from cells treated with SP600125 are impaired in their infectivity. Since JNKi-treated cells produced significantly reduced titers of infectious virus, we next wanted to examine the molecular basis of this defect. HCC cells were mock treated or exposed to SP600125 or IFN-α/β overnight, followed by infection with rVSV-GFP. Viral titers as well as the RNA copy numbers in infected supernatants were measured. The number of budded viral particles was extrapolated by real-time PCR through the quantification of genomic viral RNA and compared to the correspond-
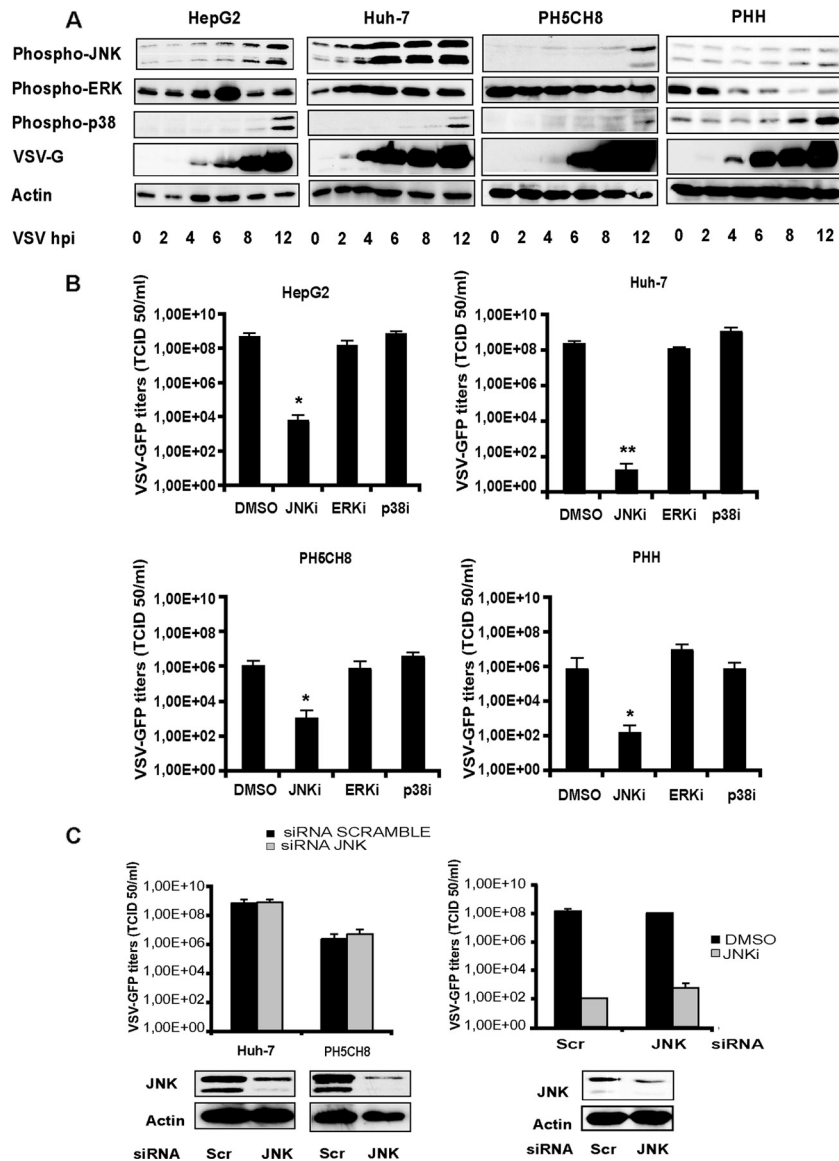
FIG 1 Activation of MAPK signaling in VSV-infected cells. (A) HCC cell lines (HepG2 and Huh-7), nonneoplastic primary hepatocytes (PH5CH8), and primary human hepatocytes (PHH) were infected with rVSV-GFP at an MOI of 10. The activation of JNK, ERK, and p38 MAPK was monitored at different time points postinfection by Western blotting via the detection of phosphorylated forms of the indicated kinases. (B) HCC cells, PH5CH8 cells, and PHH were mock treated (DMSO) or treated with SP600125 (JNKi) (25 μM), U0126 (ERKi) (10 μM), or SB203580 (p38i) and then infected with wild-type VSV at an MOI of 0.1 for 16 h. Error bars indicate standard deviations of data from experiments performed in triplicates. For all cell types, a statistically significant decrease of viral titers in SP600125-treated cells was observed (∗, $P < 0.05$; ∗∗, $P < 0.01$). (C) HCC cells (data for Huh-7 cells are shown as representative data) and PH5CH8 cells were transfected with scramble siRNA (Scr) or JNK-specific siRNA. (Left) At 72 h posttransfection, cells were infected with wild-type VSV at an MOI of 0.1 for 16 h, and viral titers in the culture supernatants were determined by TCID$_{50}$ analysis. To confirm the siRNA knockdown, cell lysates of parallel uninfected cultures were subjected to Western blot analysis using an antibody specific for JNK. (Right) HepG2 cells transfected with scramble or JNK siRNAs were either left untreated or treated with SP600125 (25 μM) prior to VSV infection at an MOI of 0.1. Cell supernatants were assayed for viral yields, and total lysates were subjected to Western blotting for JNK expression.

ing infectious viral titers in the same supernatants (Fig. 4A). Numbers of copies of the VSV genome were slightly reduced upon treatment with SP600125. In contrast, IFN-α/β treatment also resulted in an inhibition of viral genome replication. While VSV titers in mock- and IFN-treated cells closely reflected the genome copy numbers, the number of infectious particles was significantly lower than the viral genome copy numbers in the supernatants of cells treated with SP600125, indicating that the JNKi may have affected virus infectivity without adversely affecting overall virion

production. To determine if the loss of infectivity is due to reduced levels of incorporation of the viral proteins into budded virions, we examined the viral proteins in the culture supernatants of infected cells. Partially purified VSV from equal amounts of culture supernatants was pelleted, and levels of viral proteins in the viral pellets were analyzed by Western blotting. For cells treated with IFN-α/β, the levels of all viral proteins in the pellet were lower than those for mock-treated cells, consistent with the observed reduction in viral titers. Interestingly, in virus pellets
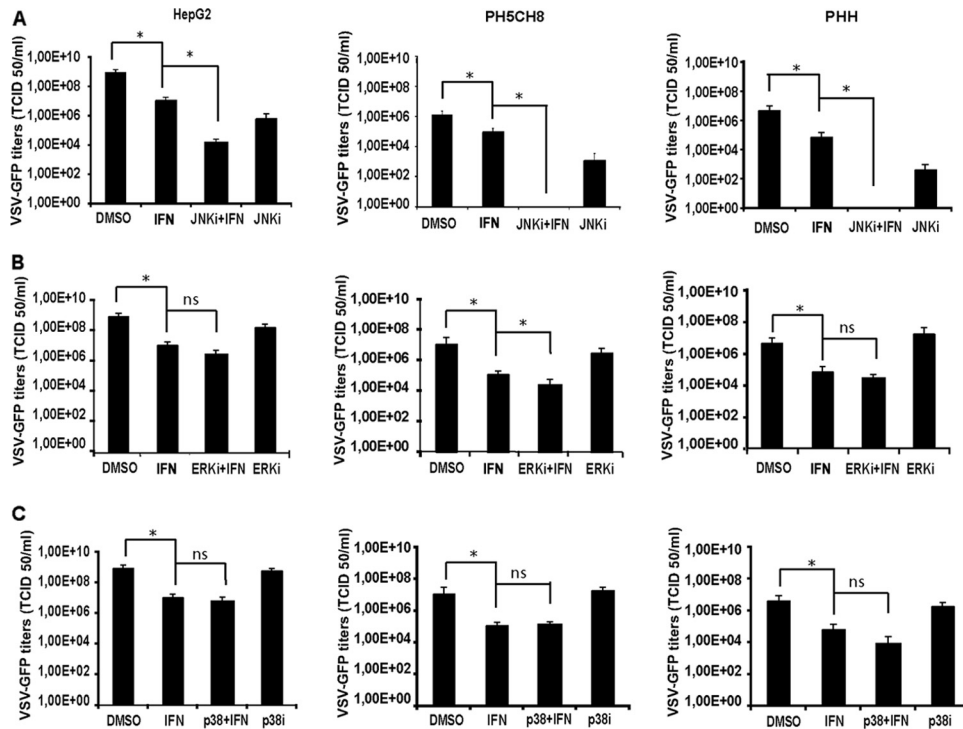
FIG 2 Antiviral activity of type I IFN in combination with MAPK inhibitors. HCC (data for HepG2 cells are shown as representative data), PH5CH8, and PHH cells were treated with IFN-α/β (100 IU/ml) in combination with 25 μM SP600125 (JNKi) (A), 10 μM U0126 (ERKi) (B), and 10 μM SB203580 (p38i) (C). Treatments with single agents and DMSO were included as controls. Infection with VSV-GFP at an MOI of 0.1 was then performed for 16 h, and viral titers were determined by TCID$_{50}$ analysis. Means of data from triplicate experiments are presented, with error bars indicating the standard deviations. Significance was determined by comparison with titers of control cultures (DMSO). ∗, $P < 0.05$; ns, nonsignificant.

from SP600125-treated cells, despite a significant reduction in VSV titers, the amount of VSV proteins was comparable to or higher than the levels in control cells (Fig. 4B). This result indicates that the loss of infectivity was not due to reduced levels of incorporation of viral G or other proteins into the budded virions. Most interestingly, the protein profile of virions produced from cells treated with SP60025 revealed an additional major protein band (identified as VSV-G*) of approximately 120 kDa, which appears to be related to the G protein (see below).

Moreover, to determine if the reduction of VSV growth in cells treated with the JNK inhibitor was due merely to differences in viral growth kinetics and, in particular, to a delay in particle release, we performed growth kinetics analyses. HCC cells were infected with VSV in the presence of vehicle (DMSO) or SP600125. Viral titers in the supernatants were determined at various times postinfection. A reduction of VSV replication in the presence of SP600125 was clearly observed during the entire duration of the kinetic analysis (Fig. 4C).

SP600125 alters VSV-G posttranslationally and hampers its fusogenic activity. As briefly described above, the purified virions and cell lysates from infected cells produced a slower-migrating band of about 120 kDa (VSV-G*), in addition to the normal G protein band, which appeared consistently when SP600125 was applied to the cells (Fig. 5A). This slower-migrating protein band was detected in infected cells or culture supernatants only in the presence of SP600125. As this additional band was specifically recognized by the antibody against VSV-G, we considered that it might represent a modified form of viral glycoprotein G. Addi-

tionally, this modified protein (VSV-G*) was also incorporated into the virions (Fig. 5A). Further studies revealed that the ectopic expression of the G protein in plasmid-transfected cells in the presence of JNKi also resulted in the appearance of this higher-molecular-weight protein band (Fig. 5B), indicating that the presence of the inhibitor may be responsible for the appearance of VSV-G* in virus-infected or plasmid-transfected cells. The sizes and levels of the other viral proteins were similar in untreated and SP600125-treated supernatants (Fig. 5C), indicating that SP600125 specifically induced the formation of this modified G protein. The anti-VSV antibody used in this experiment also detected the additional high-molecular-weight band. The presumptive modified viral glycoprotein (VSV-G*) was further analyzed by mass spectrometry. The fragments obtained after limited proteolysis could be identified as VSV-G protein peptides; no cellular proteins were consistently identified in VSV-G* preparations from two independent experiments (Table 1).

The effects of different reducing and denaturing agents were tested in an attempt to determine the nature of VSV-G*. Initially, we treated VSV-G* with dithiothreitol (DTT), a strong reducing agent, to assess the possible role of a disulfide bond in VSV-G* stability. Semipurified viral particles obtained from SP600125-treated cells were exposed to DTT prior to analysis by SDS-PAGE. Compared to samples treated with classical Laemmli buffer, containing 5% beta-mercaptoethanol and 2% SDS, DTT did not alter the stability or mobility of VSV-G* (Fig. 5D, left). Aliquots of lysates were then incubated at a different acidic pH and incubated at 4°C or preheated for 10 min at 65°C or 96°C. VSV-G* expres-
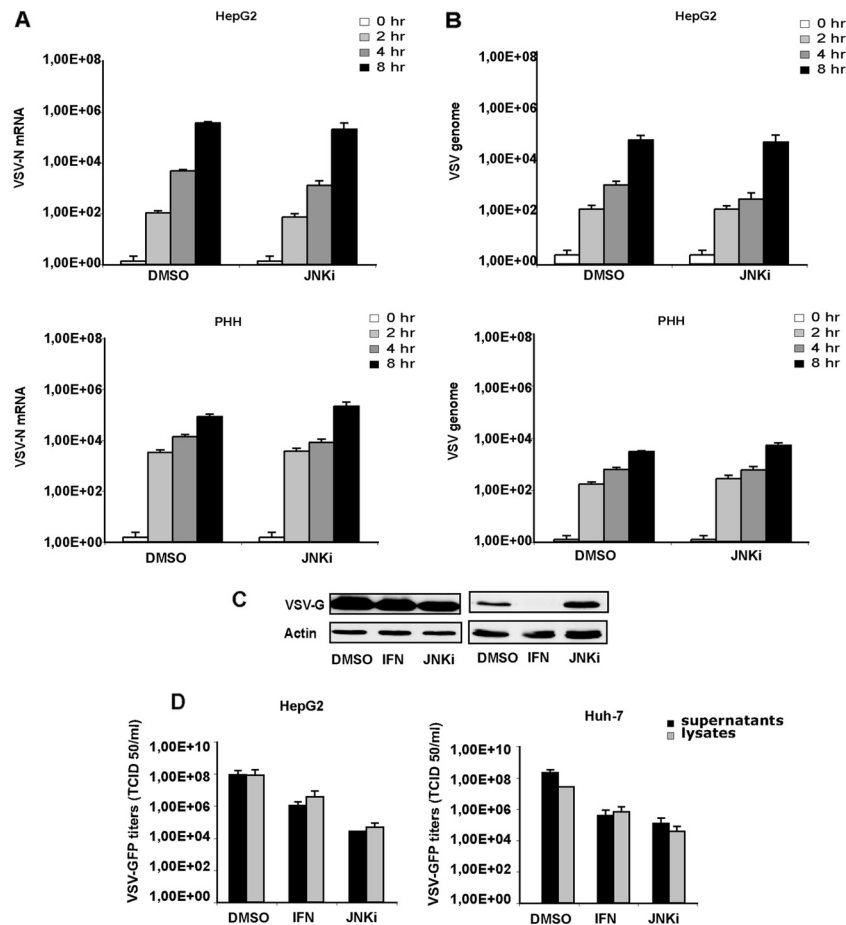
FIG 3 Viral transcription/translation and budding are not affected by SP600125. HepG2 cells and PHH were infected with VSV-GFP, and RNA was extracted at the indicated time points. (A and B) Viral mRNA for the N protein (A) and genome RNA (B) were quantified by real-time PCR. Data represent the means of data from three independent experiments. (C) Expression levels of VSV-G obtained from infected HepG2 cells and PHH previously treated with SP600125 (JNKi) or interferon (IFN) or left untreated were analyzed by Western blotting. (D) HCC cells left untreated (DMSO) or treated with SP600125 (JNKi) or IFN were infected with VSV-GFP for 16 h. Viral titers in the supernatants and corresponding cell lysates were quantified by TCID$_{50}$ analysis. Results represent the means of data from three independent experiments performed in duplicates.

sion was not affected by any of these treatments (data not shown). Additionally, to test a potential role of strong hydrophobic interactions in the VSV-G modification, the sensitivity of VSV-G* to urea treatment was analyzed. The exposure of SP600125-derived virions to 8 M urea did not affect the expression levels of both VSV-G and VSV-G*, as shown by Western blotting (Fig. 5D, right).

To exclude the possibility that SP600125 has the potential to cross-link the VSV glycoprotein, semipurified virions obtained from untreated cells were subjected either to direct exposure to SP600125 or to paraformaldehyde (PFA) (Fig. 6A). Samples were resolved by SDS-PAGE and detected by immunoblotting using an anti-VSV-G antibody. As shown in Fig. 6A, VSV-G could be cross-linked into species migrating at the molecular weight expected for dimeric and trimeric forms of the glycoprotein only upon treatment with PFA. This resulted in a drastic reduction in virus infectivity. However, the virions incubated with SP600125 retained their infectivity. Furthermore, when cells underwent pretreatment with only SP600125 and viral infection was allowed to proceed in the absence of the inhibitor, VSV growth was rescued. VSV-G* was still detectable in the corresponding cell lysates but at

much lower expression levels than in control samples, where infection was carried out in the constant presence of the inhibitor (Fig. 6B).

Alterations of envelope glycosylation were shown previously to lead to impaired virus infectivity (58). To test the hypothesis that VSV-G* could be a hyperglycosylated form of wild-type VSV-G, we subjected semipurified virions to PNGase F or to EndoGalNAcase digestion, and we monitored the effect by Western blot analysis. PNGase F cleaves N-oligosaccharides from the glycoprotein, and EndoGalNAcase releases O-linked glycans instead. Both VSV-G and VSV-G* were susceptible to PNGase F digestion, which resulted in a shift to lower-molecular-weight proteins (Fig. 6C, left), whereas EndoGalNAcase had no effect on both protein species despite the extended incubation time (Fig. 6C, right). Notably, the enzyme treatments failed to shift VSV-G* to the fully deglycosylated form.

To determine if VSV-G* could compromise the functionality of the viral glycoprotein reducing infectivity of the virions, we assessed the ability of transfected VSV-G to induce syncytia in the presence of SP600125. Huh-7 cells were transfected with a plasmid encoding the VSV G protein, and at 8 h posttransfection,
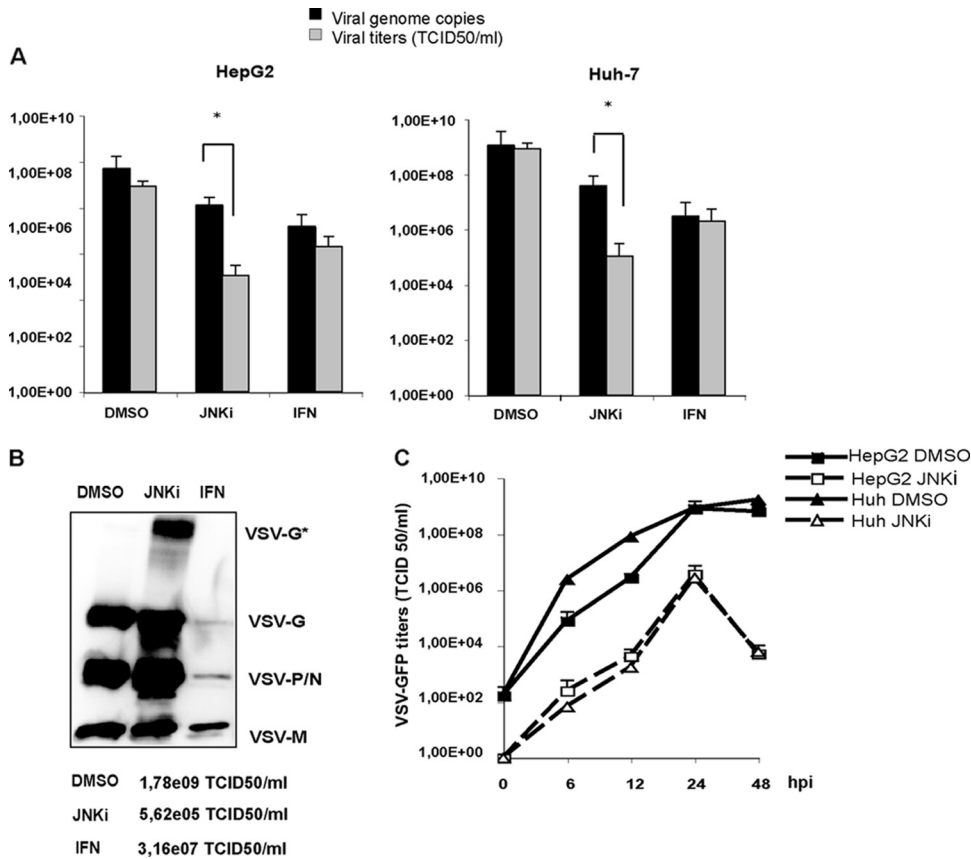
FIG 4 The JNK inhibitor SP600125 interferes with VSV infectivity. (A) Viral titers obtained from DMSO-, SP600125 (JNKi)-, and IFN-treated cells were compared to the corresponding genome copy numbers. Infection was performed for 16 h, and viral genomic RNA in the supernatants was analyzed by real-time PCR, whereas the viral titer was determined by $TCID_{50}$ assay. Upon treatment with SP600125, the difference between viral titers and genome copy numbers was significant (*, $P < 0.05$). (B) Semipurified viruses obtained from DMSO-, SP600125 (JNKi)-, and IFN-treated cell supernatants by ultracentrifugation were used to determine VSV protein expression by Western blotting. Viral titers of the samples shown are listed at the bottom. (C) Determinations of growth kinetics on HCC cells were performed in the presence of vehicle (DMSO) or SP600125 (JNKi). Cells were infected with VSV at an MOI of 0.1, and viral titers were determined by $TCID_{50}$ analysis at the indicated time points. Mean values and standard deviations from triplicate experiments are shown.

the cells were treated either with DMSO or with SP600125. The extent of syncytium formation was quantified at 24 h posttransfection by using a syncytium index (SI) (Fig. 7A, left). Syncytium formation was also visualized in transfected cells not treated (DMSO) or treated with SP600125 (JNKi) by the staining of nuclei with propidium iodide (Fig. 7A, right) The fusion activity of VSV-G in the presence of the JNK inhibitor was significantly reduced. The VSV growth attenuation in HCC cells was proportional to the concentration of SP600125 (Fig. 6B). The decrease in viral titers correlated directly with the level of expression of VSV-G* in infected cells; at a concentration of 25 μM, VSV growth was attenuated by about 10,000- to 100,000-fold, while VSV-G* was maximally expressed (Fig. 6C). Levels of the wild-type VSV G and M proteins remained unchanged.

DISCUSSION

VSV is an oncolytic virus, which selectively grows and kills a variety of cancer cells and shows an attenuated growth phenotype in normal cells. VSV selectivity is achieved by exploiting molecular defects in cancer cells, which compromise the innate antiviral defense or, on the other hand, create advantages for malignant growth and survival (38, 45). The potent cytolytic properties of

VSV in conjunction with its rapid replication cycle have made VSV an extremely promising candidate for oncolytic virotherapy (1, 31, 43, 52). Interestingly, many of the signaling pathways that viruses use are the same ones deregulated during malignant evolution. Due to their relevance in oncogenesis, these same pathways have become targets for anticancer drug development. Now that oncolytic viruses are finally entering the clinic, the time has come to take a further step forward and explore possible new application strategies involving the most up-to-date and refined anticancer agents. Therefore, it is reasonable to foresee the great potential of synergistic combinations of oncolytic viruses and small cell-permeable inhibitors of protein kinases to enhance tumor killing. For example, the various MAPK pathways (ERK1/2, JNK, and p38 MAPK) appear to be some of the most significant cellular signaling cascades in the development of several malignancies, including HCC (36, 47, 49). Therefore, the inhibition of ERK can be useful to control the growths of several human cancers (40), while JNK modulators are able to induce cancer cell death or sensitize tumor cells to apoptotic stimuli (12, 41). The JNK pathway has also been linked to cell cycle progression and antiviral responses (3, 13, 22, 42). In addition, the MAPK pathways play an important role in the life cycles of certain viruses (10, 19, 33, 46, 61). In view
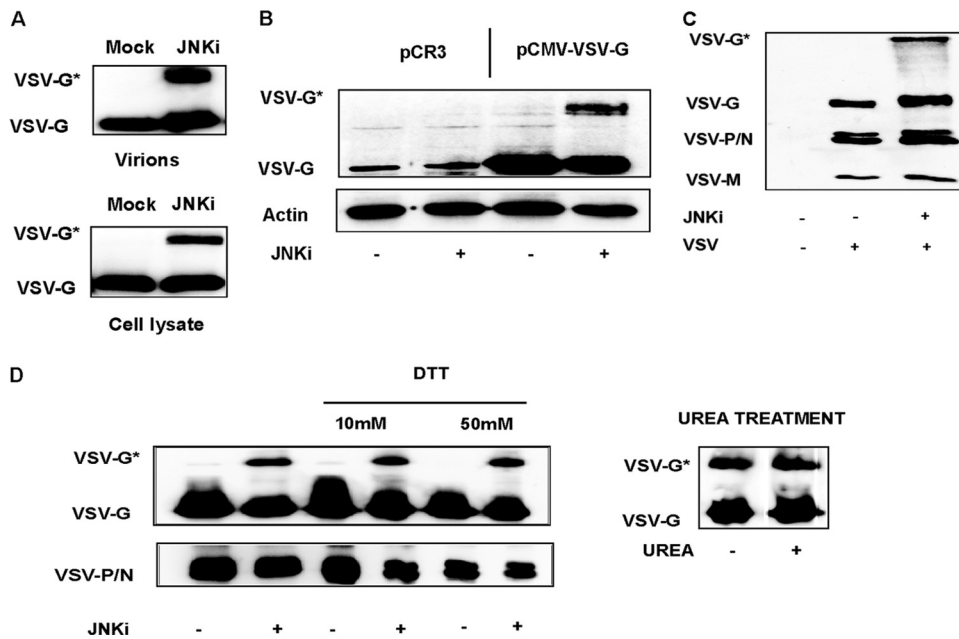
FIG 5 SP600125 induces a posttranslational modification of the VSV-G protein. (A) Levels of viral glycoprotein (VSV-G) from isolated viral particles (top) or infected-cell lysates (bottom) were analyzed by Western blotting. Huh-7 cells, used as representative cells, were pretreated with SP600125 (JNKi) or with the vehicle (DMSO) and infected with VSV at an MOI of 0.1 for 24 h. A fast-migrating band (VSV-G) was identified in all the samples and represents the mature form of the VSV glycoprotein. When infection was performed in the presence of SP600125, a slower-migrating band (VSV-G*) was present. (B) Huh-7 cells were transfected with an empty vector (pCR3) or with a vector expressing the VSV glycoprotein (pCMV-VSV-G). Cells were cultured for 24 h in the presence of DMSO or SP600125 (JNKi), and cell lysates were analyzed by Western blotting using a specific anti-VSV-G antibody. (C) Western blot analysis of VSV obtained from DMSO-treated or SP600125-treated (JNKi) cells. Levels of the VSV glycoprotein (G), phosphoprotein/nucleoprotein (P/N), and matrix protein (M) were detected by an anti-VSV serum (kindly provided by Douglas Lyles). (D) Semipurified VSV obtained from DMSO- or SP600125-treated cultures was subjected to DTT reduction. (Left) Lysates were treated with 10 or 50 mM DTT and loaded together with untreated controls on an SDS-PAGE gel. (Right) The same samples were alternatively exposed to 8 M urea and analyzed by Western blotting.

of a combinatorial approach with new drugs based on the specific targeting of MAPK and oncolytic viruses, we investigated the use of such combinations using VSV in the context of HCC.

In this work, we have studied the influence of three of the major MAPK inhibitors on VSV oncolysis *in vitro*, comparing HCC cell lines with primary human hepatocytes. It was previously shown that ERK facilitates VSV-mediated oncolysis by the nega-

tive regulation of the IFN-α response (43). In many HCC cell lines, the innate immunity response to pathogens is compromised, especially due to multiple defects in the type I IFN system (38). The reestablishment of a functional type I IFN response in HCC would be seriously detrimental to the therapeutic efficacy of VSV. Our studies demonstrated that in HCC cell lines, the activation of the ERK signaling pathway does not enhance VSV oncol-

TABLE 1 Identification of SP600125-induced high-molecular-mass VSV-G* by MS

| Positions of fragment	Expected mass (kDa)	Measured mass (kDa)	Δ mass	No. of misses	Sequence
1–11	1,357.84	1,357.75	0.09	1	KFTIVFPHNQK
16–44	3,328.6	3,328.56	0.04	0	NVPSNYHYCPSSSDLNWHNDLIGTAIQVK
51–63	1,489.70	1,489.64	0.05	0	AIQADGWMCHASK
84–100	1,996.93	1,996.94	−0.01	1	SFTPSVEQCKESIEQTK
175–200	2,834.21	2,834.30	−0.09	0	GLCDSNLISMDITFFSEDGELSSLGK
207–217	1,235.50	1,235.55	−0.05	0	SNYFAYETGGK
231–249	2,123.14	2,123.05	0.09	1	LPSGVWFEMADKDLFAAAR
250–277	3,033.54	3,033.42	0.12	0	FPECPEGSSISAPSQTSVDVSLIQDVER
278–290	1,641.85	1,641.77	0.08	0	ILDYSLCQETWSK
293–308	1,639.91	1,639.91	−0.01	0	AGLPISPVDLSYLAPK
333–342	1,053.55	1,053.62	−0.07	0	VDIAAPILSR
343–354	1,313.58	1,313.60	−0.01	0	MVGMISGTTTER
355–375	2,472.19	2,472.16	0.04	0	ELWDDWAPYEDVEIGPNGVLR
382–401	2,292.10	292.09	0.01	0	FPLYMIGHGMLDSDLHLSSK
402–432	3,398.62	3,398.61	0.01	0	AQVFEHPHIQDAASQLPDDESLFFGDTGLSK
433–446	1,690.87	1,690.84	0.03	0	NPIELVEGWFSSWK
483–492	1,297.53	1,297.60	−0.07	0	QIYTDIEMNR
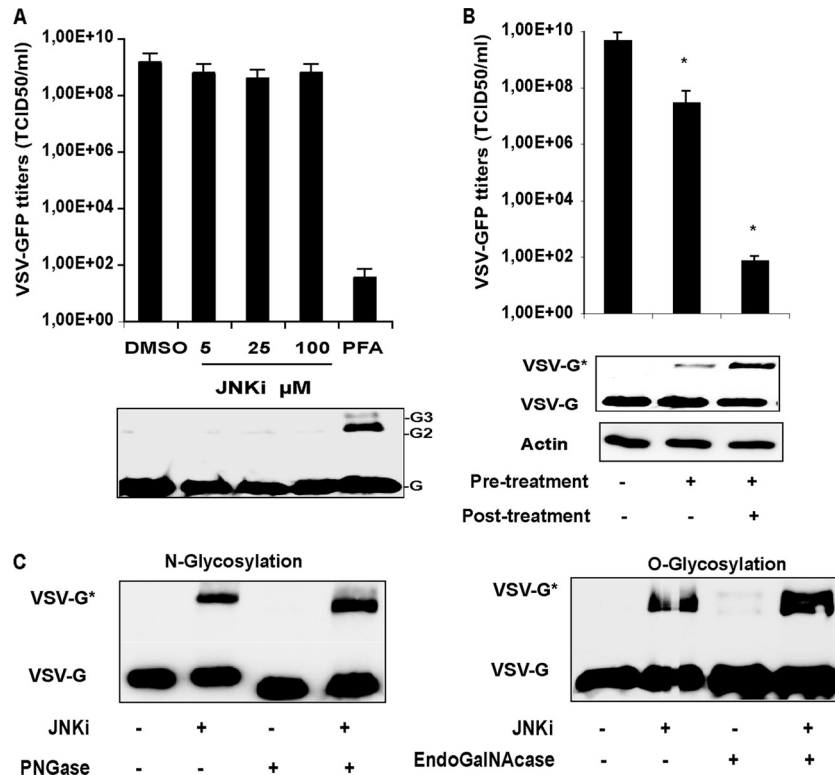
FIG 6 VSV-G* is not the result of cross-linking or hyperglycosylation processes. (A) Semipurified virions were exposed to increasing concentrations of SP600125 (JNKi) for 1 h on ice. As a control, virions were cross-linked with PFA (2%) on ice for 15 min. One-tenth of the samples was preheated at 56°C for 10 min and loaded onto an SDS-PAGE gel. Viral glycoprotein monomers (G), dimers (G2), and trimers (G3) were detected with a polyclonal antibody specific for VSV-G (bottom). The same samples were used to infect HepG2 cells, and viral progeny was quantified by TCID$_{50}$ analysis at 24 h postinfection. (B) Huh-7 cells were pretreated with SP600125 and infected with VSV-GFP at an MOI of 1. Infection was carried out without or in the presence of the inhibitor SP600125 for 24 h. DMSO-treated cells were used as a control. Viral titers and levels of VSV-G and VSV-G* in the corresponding cell lysates are shown and represent the means of data from three independent experiments. (C) Semipurified virions obtained in the presence or absence of SP600125 were digested with PNGase F (left) or EndoGalNAcase (right) overnight. After digestion, the expression levels of VSV-G and VSV-G* were analyzed by Western blotting.

ysis, since protection from lytic infection was not improved by the coadministration of the ERK inhibitor U0126 and IFN-α/β. Therefore, the disruption of ERK signaling by anticancer drugs seems to be compatible with VSV therapy in HCC, at least *in vitro*. The discrepancy of our results compared with those of previous reports (43) emphasizes the need to consider each cancer type as a unique environment. For this reason, preliminary *in vitro* studies assume a great significance in view of subsequent clinical investigations.

Since their discovery in the early 1990s, JNKs have attracted intense interest due to the increasing evidence of the involvement of JNK-dependent signaling events in the development of several pathological conditions. The potential therapeutic application of JNK-specific inhibitors for the treatment of different human diseases, from ischemia, diabetes, and cancer to viral infectious diseases, has been explored (25, 34, 39). Notably, JNK1 has an essential oncogenic role in HCC development, and direct evidence comes from *in vivo* studies with JNK1 knockout mice. In mice lacking JNK1, diethylnitrosamine-triggered liver tumorigenesis was remarkably reduced, and treatment with chemical JNK inhibitors resulted in the reduced growth of xenografted human HCC cells (22, 42). Besides SP600125 (3), several small-molecule compounds inhibiting JNK kinase activity with higher selectivity and efficacy have been developed (35), and the combination of these

new inhibitors with VSV virotherapy could potentially be beneficial for HCC treatment.

Increasingly, it has been shown that viral infection can lead to stress-activating protein kinase (SAPK)/JNK and p38 MAPK activation, which is needed for viral replication and release (21, 39, 54, 61). In this report, we observed a strong activation of JNK upon the infection of HCC cell lines with VSV, while the levels of activation of ERK and p38 MAPK were very weak. Inhibitors of p38 MAPK (SB203580) and of ERK (U0126) did not reduce the viral yield in HCC cells. On the other hand, the JNK inhibitor SP600125 dramatically decreased viral titers in all cell types tested, consistent with previous studies with dengue virus, rotavirus, and circovirus (7, 19, 56). SP600125 and other similar anthrapyrazoles are considered to be valuable therapeutic agents; their usefulness against cancer (3, 15), liver injury, and fibrosis (20, 29) has been associated with minimal toxicity *in vivo*. Unfortunately, in light of our results, we excluded the possibility of a conjunctive application of SP600125 and VSV therapy. However, our results indicate that the attenuation of VSV by SP600125 is due to a nonspecific mechanism that does not involve the inhibition of JNK, and therefore, the combination of VSV and other specific JNK inhibitors still represents a viable treatment option.

Most interestingly, despite the fact that the numbers of copies of the viral genome in the supernatants of SP600125-treated cells
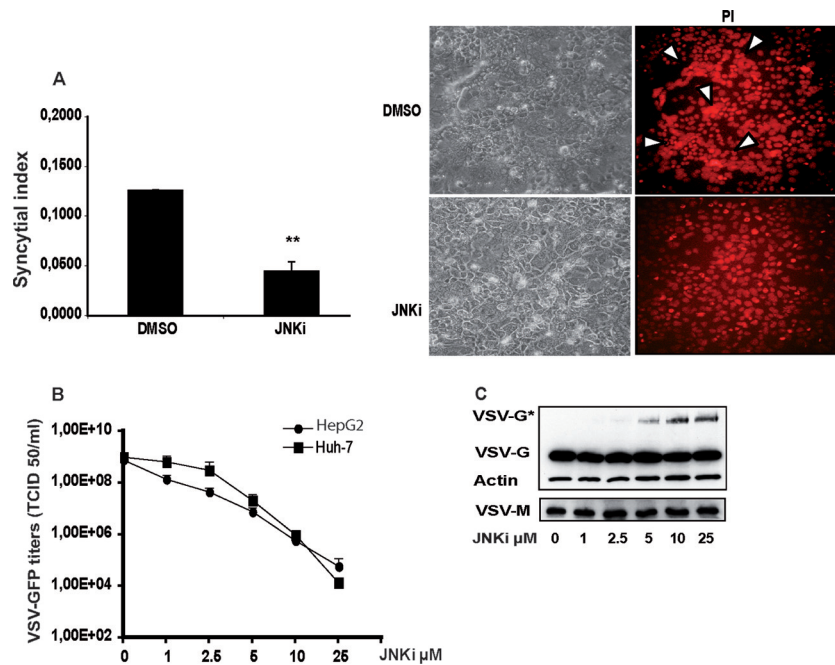
FIG 7 SP600125 decreases the fusion activity of VSV-G. (A) Huh-7 cells were transfected with an expression vector for the VSV glycoprotein (pCMV-VSV-G). At 8 h posttransfection, supernatants were replaced with fresh medium containing either DMSO or SP600125 (25 μM). Syncytium formation was quantified by the determination of the syncytium index (SI) (Fig. 6A, left), and parallel cultures were fixed and stained with propidium iodide (PI) to visualize syncytia (Fig. 6A, right). $**$, $P < 0.01$. (B) HCC cells were treated with increasing concentrations of SP600125 and infected with VSV at an MOI of 0.1 for 24 h. Aliquots of the supernatants were subjected to $TCID_{50}$ assay for determination of viral titers. Means and standard deviations of data from duplicate experiments are shown. (C) Expression levels of VSV-G and VSV-G* were analyzed by Western blotting in the corresponding cell lysates (data for HepG2 cells are shown as representative data). The maximum expression level of VSV-G* was at 25 μM SP600125, the concentration which corresponds to the greatest attenuation of VSV.

did not differ substantially from those in the untreated controls, the infectious viral titers were significantly lower, up to 10,000- to 100,000-fold. These results led us to conclude that SP600125 affects VSV infectivity such that only a fraction of the new viral progeny released into the culture supernatant retains the ability to reinfect cells. As a cause of a lack of infectivity of newly formed virions, we have found that the viral particles incorporate at least two different forms of the G protein in the presence of SP600125: one that comigrates with the normal G protein and the other that is significantly higher in molecular mass than the normal G protein (VSV-G*). The same result was observed when a VSV-G protein-expressing plasmid was transfected in the presence of the JNK inhibitor.

At this point, we speculated that VSV-G* could represent either a hyperglycosylated form of VSV-G or a VSV-G dimer, since the size was roughly twice the size of the monomeric G protein. An alteration of glycosylation can have a dramatic impact on the infectivity of viruses; as observed previously by Whitt and colleagues, virions incorporating a glycoprotein with an additional N-linked oligosaccharide in the extracellular domain were not infectious, apparently due to the formation of heterodimers that lacked fusion activity (58). In our experiments, digestion with *N*- or *O*-glycosidases did not completely abolish VSV-G* expression, leading us to the conclusion that this form was not assignable to a hyperglycosylated status (Fig. 6C). Intriguingly, VSV-G* may represent a protein complex or an as-yet-unknown modification of the G protein that is thermostable and resistant to SDS; additionally, it does not dissociate under reducing conditions (DTT) and is not denatured by urea. Moreover, exposure to an acidic pH at an

elevated temperature did not to affect the detection of VSV-G* (data not shown).

The incubation of extracellular VSV with SP600125 did not lead to VSV-G* formation, nor did it hamper viral infectivity, ruling out a possible cross-linking activity of SP600125. Pretreatment alone with infection carried out in the absence of SP600125 resulted in reduced levels of VSV-G* and a partial recovery of viral titers.

Mass spectrometry analysis revealed that VSV-G* contains only peptides from the VSV G protein. In repeated experiments, we did not identify any cellular protein consistently in VSV-G* preparations, including the ones related to major posttranslational modifications, such as ubiquitination, sumoylation, neddylation, and ISGylation, etc. (23, 27, 50, 55, 59). Despite the fact that we were able to exclude several mechanisms involved in protein modifications, the nature of VSV-G* still remains enigmatic, yet it is possible that unidentified modifications through covalent linkages are responsible for the formation of VSV-G*. Given the difficulty in identifying these processes, further studies will be required to address this important aspect.

The presence of VSV-G* species compromised the fusion activity of the VSV glycoprotein; in the presence of SP600125, the expression of VSV-G* led to a reduction in levels of syncytium formation. Since increased levels of VSV-G* expression depend on the SP600125 concentration and correlate inversely with viral titers, we postulate that SP600115 attenuates VSV by hampering the VSV glycoprotein fusogenic activity.

In conclusion, our *in vitro* results support the concept that combination therapy using oncolytic VSV and MAPK inhibitors

might result in synergistic antitumor activity against HCC, and we plan to test this hypothesis in future *in vivo* studies. Furthermore, at the molecular level, we have provided new insights into the antiviral properties of the inhibitor SP600125. SP600125 also attenuates the growths of several viruses of different families, suggesting a possible common mechanism of action that could be exploited for the development of antiviral treatment. A very intriguing application of SP600125 could be as a treatment of viral infections that are accompanied by malignant transformation. Both antiviral and antitumor effects of the drug could have significant benefits, for example, in the treatment of hepatitis C virus or human papillomavirus infection (16, 60). The elucidation of viral posttranslational control and viral mechanisms of infectivity can also be investigated by means of the effect of SP600125 on VSV-G maturation, leading to the development of new and targeted antiviral strategies.

ACKNOWLEDGMENTS

REFERENCES

1. **Altomonte J, et al.** 2008. Synergistic antitumor effects of transarterial viroembolization for multifocal hepatocellular carcinoma in rats. Hepatology **48**:1864–1873.
2. **Banerjee S, et al.** 2008. Hepatitis C virus core protein upregulates serine phosphorylation of insulin receptor substrate-1 and impairs the downstream Akt/protein kinase B signaling pathway for insulin resistance. J. Virol. **82**:2606–2612.
3. **Bennett BL, et al.** 2001. SP600125, an anthrapyrazolone inhibitor of Jun N-terminal kinase. Proc. Natl. Acad. Sci. U. S. A. **98**:13681–13686.
4. **Bode AM, Dong Z.** 2007. The functional contrariety of JNK. Mol. Carcinog. **46**:591–598.
5. **Bogoyevitch MA.** 2006. The isoform-specific functions of the c-Jun N-terminal kinases (JNKs): differences revealed by gene targeting. Bioessays **28**:923–934.
6. **Cargnello M, Roux PP.** 2011. Activation and function of the MAPKs and their substrates, the MAPK-activated protein kinases. Microbiol. Mol. Biol. Rev. **75**:50–83.
7. **Ceballos-Olvera I, Chavez-Salinas S, Medina F, Ludert JE, del Angel RM.** 2010. JNK phosphorylation, induced during dengue virus infection, is important for viral infection and requires the presence of cholesterol. Virology **396**:30–36.
8. **Chen F, Castranova V.** 2009. Beyond apoptosis of JNK1 in liver cancer. Cell Cycle **8**:1145–1147.
9. **Clarke P, et al.** 2004. JNK regulates the release of proapoptotic mitochondrial factors in reovirus-infected cells. J. Virol. **78**:13132–13138.
10. **Clarke P, Meintzer SM, Widmann C, Johnson GL, Tyler KL.** 2001. Reovirus infection activates JNK and the JNK-dependent transcription factor c-Jun. J. Virol. **75**:11275–11283.
11. **Corcoran JA, et al.** 2006. The p14 fusion-associated small transmembrane (FAST) protein effects membrane fusion from a subset of membrane microdomains. J. Biol. Chem. **281**:31778–31789.
12. **Dhanasekaran DN, Reddy EP.** 2008. JNK signaling in apoptosis. Oncogene **27**:6245–6251.
13. **Du L, et al.** 2004. Inhibition of cell proliferation and cell cycle progression by specific inhibition of basal JNK activity: evidence that mitotic Bcl-2 phosphorylation is JNK-independent. J. Biol. Chem. **279**:11957–11966.
14. **Ebert O, et al.** 2003. Oncolytic vesicular stomatitis virus for treatment of orthotopic hepatocellular carcinoma in immune-competent rats. Cancer Res. **63**:3605–3611.
15. **Hanajiri K, et al.** 2009. Echographic detection of diethylnitrosamine-induced liver tumors in rats and the effect of the intratumoral injection of an inhibitor of c-Jun N-terminal kinase. J. Gastroenterol. Hepatol. **24**:866–871.
16. **Hassan M, Ghozlan H, Abdel-Kader O.** 2005. Activation of c-Jun NH2-terminal kinase (JNK) signaling pathway is essential for the stimulation of hepatitis C virus (HCV) non-structural protein 3 (NS3)-mediated cell growth. Virology **333**:324–336.
17. **Heasley LE, Han SY.** 2006. JNK regulation of oncogenesis. Mol. Cells **21**:167–173.
18. **Hirasawa K, et al.** 2003. Effect of p38 mitogen-activated protein kinase on the replication of encephalomyocarditis virus. J. Virol. **77**:5649–5656.
19. **Holloway G, Coulson BS.** 2006. Rotavirus activates JNK and p38 signaling pathways in intestinal cells, leading to AP-1-driven transcriptional responses and enhanced virus replication. J. Virol. **80**:10624–10633.
20. **Hu YB, Liu XY.** 2009. Protective effects of SP600125 in a diet-induced rat model of non-alcoholic steatohepatitis. Scand. J. Gastroenterol. **44**:1356–1362.
21. **Huerta-Zepeda A, et al.** 2008. Crosstalk between coagulation and inflammation during dengue virus infection. Thromb. Haemost. **99**:936–943.
22. **Hui L, Zatloukal K, Scheuch H, Stepniak E, Wagner EF.** 2008. Proliferation of human HCC cells and chemically induced mouse liver cancers requires JNK1-dependent p21 downregulation. J. Clin. Invest. **118**:3943–3953.
23. **Isaacson MK, Ploegh HL.** 2009. Ubiquitination, ubiquitin-like modifiers, and deubiquitination in viral infection. Cell Host Microbe **18**:559–570.
24. **Iyoda K, et al.** 2003. Involvement of the p38 mitogen-activated protein kinase cascade in hepatocellular carcinoma. Cancer **97**:3017–3026.
25. **Kaneto H.** 2005. The JNK pathway as a therapeutic target for diabetes. Expert Opin. Ther. Targets **9**:581–592.
26. **Kayser JP, Vallet JL, Cerny RL.** 2004. Defining parameters for homology-tolerant database searching. J. Biomol. Tech. **15**:285–295.
27. **Kerscher O, Felberbaum R, Hochstrasser M.** 2006. Modification of proteins by ubiquitin and ubiquitin-like proteins. Annu. Rev. Cell Dev. Biol. **22**:159–180.
28. **Keshet Y, Seger R.** 2010. The MAP kinase signaling cascades: a system of hundreds of components regulates a diverse array of physiological functions. Methods Mol. Biol. **661**:3–38.
29. **Kluwe J, et al.** 2010. Modulation of hepatic fibrosis by c-Jun-N-terminal kinase inhibition. Gastroenterology **138**:347–359.
30. **Kook SH, et al.** 2008. Inhibition of c-Jun N-terminal kinase sensitizes tumor cells to flavonoid-induced apoptosis through down-regulation of JunD. Toxicol. Appl. Pharmacol. **227**:468–476.
31. **Kubo T, et al.** 2011. Oncolytic vesicular stomatitis virus administered by isolated limb perfusion suppresses osteosarcoma growth. J. Orthop. Res. **29**:795–800.
32. **Kyriakis JM, Avruch J.** 2001. Mammalian mitogen-activated protein kinase signal transduction pathways activated by stress and inflammation. Physiol. Rev. **81**:807–869.
33. **Lambert PJ, et al.** 2007. Targeting the PI3K and MAPK pathways to treat Kaposi's-sarcoma-associated herpes virus infection and pathogenesis. Expert Opin. Ther. Targets **11**:589–599.
34. **Liu JR, et al.** 2010. The c-Jun N-terminal kinase (JNK) inhibitor XG-102 enhances the neuroprotection of hyperbaric oxygen after cerebral ischaemia in adult rats. Neuropathol. Appl. Neurobiol. **36**:211–224.
35. **Liu M, et al.** 2007. Discovery of a new class of 4-anilinopyrimidines as potent c-Jun N-terminal kinase inhibitors: synthesis and SAR studies. Bioorg. Med. Chem. Lett. **17**:668–672.
36. **Llovet JM, Bruix J.** 2008. Molecular targeted therapies in hepatocellular carcinoma. Hepatology **48**:1312–1327.
37. **Lu YY, Chen TS, Wang XP, Qu JL, Chen M.** 2010. The JNK inhibitor SP600125 enhances dihydroartemisinin-induced apoptosis by accelerat-

ing Bax translocation into mitochondria in human lung adenocarcinoma cells. FEBS Lett. **584**:4019–4026.

38. **Marozin S, et al.** 2008. Inhibition of the IFN-beta response in hepatocellular carcinoma by alternative spliced isoform of IFN regulatory factor-3. Mol. Ther. **16**:1789–1797.

39. **Mizutani T, Fukushi S, Saijo M, Kurane I, Morikawa S.** 2005. JNK and PI3k/Akt signaling pathways are required for establishing persistent SARS-CoV infection in Vero E6 cells. Biochim. Biophys. Acta **1741**:4–10.

40. **Montagut C, Settleman J.** 2009. Targeting the RAF-MEK-ERK pathway in cancer therapy. Cancer Lett. **283**:125–134.

41. **Mucha SR, et al.** 2009. JNK inhibition sensitises hepatocellular carcinoma cells but not normal hepatocytes to the TNF-related apoptosis-inducing ligand. Gut **58**:688–698.

42. **Nagata H, et al.** 2009. Inhibition of c-Jun NH2-terminal kinase switches Smad3 signaling from oncogenesis to tumor-suppression in rat hepatocellular carcinoma. Hepatology **49**:1944–1953.

43. **Noser JA, et al.** 2007. The RAS/Raf1/MEK/ERK signaling pathway facilitates VSV-mediated oncolysis: implication for the defective interferon response in cancer cells. Mol. Ther. **15**:1531–1536.

44. **Nussler A, et al.** 2009. Regenerative medicine today: the holy grail of hepatocyte culturing and therapeutic use. Springer, Brighton, United Kingdom.

45. **Oliere S, et al.** 2008. Vesicular stomatitis virus oncolysis of T lymphocytes requires cell cycle entry and translation initiation. J. Virol. **82**:5735–5749.

46. **Pleschka S.** 2008. RNA viruses and the mitogenic Raf/MEK/ERK signal transduction cascade. Biol. Chem. **389**:1273–1282.

47. **Roberts PJ, Der CJ.** 2007. Targeting the Raf-MEK-ERK mitogen-activated protein kinase cascade for the treatment of cancer. Oncogene **26**:3291–3310.

48. **Salsman J, Top D, Barry C, Duncan R.** 2008. A virus-encoded cell-cell fusion machine dependent on surrogate adhesins. PLoS Pathog. **4**:e1000016.

49. **Schmidt CM, McKillop IH, Cahill PA, Sitzmann JV.** 1997. Increased MAPK expression and activity in primary human hepatocellular carcinoma. Biochem. Biophys. Res. Commun. **236**:54–58.

50. **Schwartz DC, Hochstrasser M.** 2003. A superfamily of protein tags: ubiquitin, SUMO and related modifiers. Trends Biochem. Sci. **28**:321–328.

51. **Shin EC, et al.** 2002. Human hepatocellular carcinoma cells resist to TRAIL-induced apoptosis, and the resistance is abolished by cisplatin. Exp. Mol. Med. **34**:114–122.

52. **Shinozaki K, Ebert O, Woo SL.** 2005. Eradication of advanced hepatocellular carcinoma in rats via repeated hepatic arterial infusions of recombinant VSV. Hepatology **41**:196–203.

53. **Shinozaki K, et al.** 2004. Oncolysis of multifocal hepatocellular carcinoma in the rat liver by hepatic artery infusion of vesicular stomatitis virus. Mol. Ther. **9**:368–376.

54. **Si X, et al.** 2005. Stress-activated protein kinases are involved in coxsackievirus B3 viral progeny release. J. Virol. **79**:13875–13881.

55. **Wang Y, Pernet O, Lee B.** 2012. Regulation of the nucleocytoplasmic trafficking of viral and cellular proteins by ubiquitin and small ubiquitin-related modifiers. Biol. Cell **104**:121–138.

56. **Wei L, Zhu Z, Wang J, Liu J.** 2009. JNK and p38 mitogen-activated protein kinase pathways contribute to porcine circovirus type 2 infection. J. Virol. **83**:6039–6047.

57. **Weston CR, Davis RJ.** 2007. The JNK signal transduction pathway. Curr. Opin. Cell Biol. **19**:142–149.

58. **Whitt MA, Zagouras P, Crise B, Rose JK.** 1990. A fusion-defective mutant of the vesicular stomatitis virus glycoprotein. J. Virol. **64**:4907–4913.

59. **Wimmer P, Schreiner S, Dobner T.** 2012. Human pathogens and the host cell SUMOylation system. J. Virol. **86**:642–654.

60. **Yu JH, Lin BY, Deng W, Broker TR, Chow LT.** 2007. Mitogen-activated protein kinases activate the nuclear localization sequence of human papillomavirus type 11 E1 DNA helicase to promote efficient nuclear import. J. Virol. **81**:5066–5078.

61. **Zapata HJ, Nakatsugawa M, Moffat JF.** 2007. Varicella-zoster virus infection of human fibroblast cells activates the c-Jun N-terminal kinase pathway. J. Virol. **81**:977–990.